https://doi.org/10.3311/PPme.11727

Periodica Polytechnica Mechanical Engineering, 64(3), pp. 179–188, 2020

Implementation of Linear Stability Theory on Hollow Cone-shaped Liquid Sheet

Hadiseh Karimaei[1*], Ramin Ghorbani[2], Seyed Mostafa Hosseinalipour[2]

[1] Department of Astronautics Systems, Aerospace Research Institute, Ministry of Science, Research and Technology, Mahestan street, 14668-834 Tehran, Iran
[2] Energy, Water and Environment Research Lab, Department of Mechanical engineering, Iran University of Science and Technology, P. O. B. 16765-163, 16846-13114 Tehran, Narmak, Iran
[*] Corresponding author, e-mail: karimaei@ari.ac.ir

Received: 20 November 2017, Accepted: 20 May 2020, Published online: 07 July 2020

Abstract

Surface instability of a swirling liquid sheet emanating from a centrifugal injector in presence of external and internal gas flows is studied in this paper. A three-dimensional flow for the liquid sheet and two-dimensional flows for external and internal gas flows are considered. The set of equations involved in this analysis differs from the earlier analyzes. In previous studies, a cylindrical liquid sheet has been considered to implement the linear theory but in this study, the linear stability theory is implemented on a cone-shaped liquid sheet for different cone angles. Actually more over than axial and tangential movements, the radial movements of liquid sheet and gas flows are considered in the present model. Due to complexity of the derived governing equations, semi-analytical and numerical methods were applied to solve them. The case study is oxidizer injector of rocket engines. Implementation of linear stability theory on a hollow cone-shaped liquid sheet better can predict instability phenomenon than the general linear stability analysis for this type of liquid sheets. The results show very close agreement with available experimental data.

Keywords

cone-shaped liquid sheet, linear stability theory, primary breakup, wave growing rate, wave number

1 Introduction

A liquid sheet instability and breakup which cause to atomize the liquid bulk has been applied in many industries such as combustion chambers, pharmaceutical products manufacturing, foods drying and specially rocket engines [1]. The forces on a liquid-gas interface in a spray that interacts are the inertia force, centrifugal force, viscous force, pressure and surface tension. These forces lead to grow the disturbances on the liquid sheet and finally break up it into ligaments [2]. The cause of forming these disturbances is the turbulence of internal injector flow. Spray formation and its characteristics are also controlled by the liquid sheet instability. Subsequent phenomena such as phase transform and heat/mass transfer processes are affected by the spray characteristics.

Rayleigh [3], as a pioneer, classically studied about the liquid jets and sheets instability. Crapper et al. [4] analytically investigated an annular liquid sheet instability. They parametrically studied the effect of sheet characteristics on the wave growing rate and showed the growing rate of asymmetric and symmetric disturbances increases with decreasing inner radius. They concluded when the sheet thickness decreases, the annular liquid jet with symmetric disturbances becomes less unstable whereas with asymmetric disturbances becomes more unstable. Shen and Li [5] experimentally measured the breakup length and droplet size of an annular liquid spray with the involvement of the external and internal gas flows. They showed that a thin annular liquid sheet breaks up faster than a plane one. Panchagnula et al. [6] employed a linear technique to study the instability of a swirling annular liquid sheet exposed to the different-velocity gases. The effect of viscosity on the liquid sheet instability (symmetric mode) with same-velocity external and internal gas flows were studied by Jeandel and Dumouchel [7]. An experimental study about the sheet breakup and the spray formation has been early done for a planar nozzle designed by Jazayeri and Li [8]. Chin et al. [9] experimentally studied the effect of gas flows direction swirling

Cite this article as: Karimaei, H., Ghorbani, R., Hosseinalipour, S. M. "Implementation of Linear Stability Theory on Hollow Cone-shaped Liquid Sheet", Periodica Polytechnica Mechanical Engineering, 64(3), pp. 179–188, 2020. https://doi.org/10.3311/PPme.11727

relative to the liquid jet on the instability for high-pressure air-blast atomizers. They showed that the smallest droplets can be formed using counter-external and co-internal gas flows relative to the liquid jet. Sirignano and Mehring [10] published a dependable review on breakup of unstable liquid jets and sheets. They studied planar sheets and cylinder-shaped liquid jets with swirling and axial velocity distributions. Correspondingly Lin [11] presented a note about that. Cao [12] employed the linear stability theory on an annular liquid sheet to investigate the influence of velocity of external and internal gas flows on the breakup process of liquid sheet. Du and Li [13] studied the effect of swirling velocities of external and internal gases on the instability of liquid sheet. Ibrahim [14] inclusively studied the linear and nonlinear instability waves on an annular jet subject to the external and internal gas flows (axial velocity). He parametrically studied the effect of different factors like liquid and gas axial Weber numbers, liquid and gas swirl Weber numbers, jet thickness and gas-liquid density ratio on the wave growing rate which is a function of wave number. After that, Ibrahim and Jog [15] worked on nonlinear instability of a liquid sheet. They determined the breakup time in terms of the gas-to-liquid velocity ratio, gas swirl strength and liquid Weber number. Sahu and Matar [16] considered the three-dimensional linear stability characteristics of pressure-driven two-layer channel flow. Their results demonstrated the presence of three-dimensional instabilities for situations where the square root of the viscosity ratio is larger than the thickness ratio of the two layers. They also showed that the "shear" modes, which are present at sufficiently large Reynolds numbers, are most unstable to two-dimensional disturbances.

Yan et al. [17] considered the effect of viscosity in the nonlinear stability analysis of a liquid sheet and showed that disturbances growth becomes slow and breakup length and time increase by considering liquid viscosity. Also Mahdavi et al. [18] estimated the breakup length of a round and an annular liquid sheet by implementing the linear stability theory formulated by Ibrahim [14]. Fu et al. [19] used a linear stability analysis method to investigate the breakup of a conical liquid sheet, but they did not consider the radial velocity in the analysis and also they did not get involved the spray cone angle directly in governing equations [19]. Sahu and Govindarajan [20] studied the stability of two-fluid flow through a plane channel at Reynolds numbers of 100–1000 in the linear and nonlinear regimes. The two fluids have the same density but different viscosities. They showed that the stability of the flow is moderately sensitive to the location of the interface between the two fluids. As expected, flow at higher Reynolds numbers is more unstable.

In the current study, to achieve the most unstable wave growing on the liquid sheet earlier than break-up the linear stability theory is used. It should be mentioned that the set of equations involved in this analysis differs from the earlier analyzes. In earlier studies the linear stability analysis had been implemented on a cylindrical liquid sheet but in the present study, linear stability analysis is implemented on a cone-shaped liquid sheet by considering radial velocities of liquid sheet and gas flows and the spray cone angle [14–18]. Modeling of a hollow cone liquid jet has a lot of difficulties and involves a lot of parameters. The first one is the thickness of sheet changing to the downstream side. Additional problem that makes the technique more difficult is considering the cone angle in governing equations. The stability analysis can be enhanced by involving the mentioned factors in governing equations, and the further truthful results can be obtained. Here, actually more over than axial and tangential movements, it should be considered radial movements of the gas flows and liquid sheet. The main purpose of this study is to investigate the ability of the recommended implementation of linear stability theory for prediction of spray breakup length and properties of waves on them.

2 Implementation of linear stability theory on a hollow cone-shaped liquid sheet

Fig. 1 shows an annular swirling liquid sheet exposed to the gas flows which has been deliberated for the stability analysis in the current work. However, early studies, according to Fig. 2, had considered a cylinder-shaped liquid sheet to analyze the instability phenomenon [14–18]. But in the current paper the linear stability analysis is implemented on a cone-shaped liquid sheet and, therefore, the influence of cone angle is considered in estimations. Both phases are assumed incompressible and inviscid. Jeandel and Domouchel [7] concluded that the effect of viscosity can be ignored for an annular sheet when $\mathrm{We}_g^2 / \mathrm{Re}$ is smaller than 10^{-3} ($\mathrm{We}_g = \rho_g U_l^2 h_c / \sigma$). Also Liao et al. [21] showed that for the Reynolds number larger than 100 assuming inviscid sheet is correct. In this study, this parameter is below 10^{-4}, therefore, assuming the inviscid sheet is correct. As well, gas viscous shear is not considered in the modeling of Gordillo and Pérez-Saborid [22] because $\mu_g / \mu_l \ll 1$. Thus the viscosities of both phases are neglected.

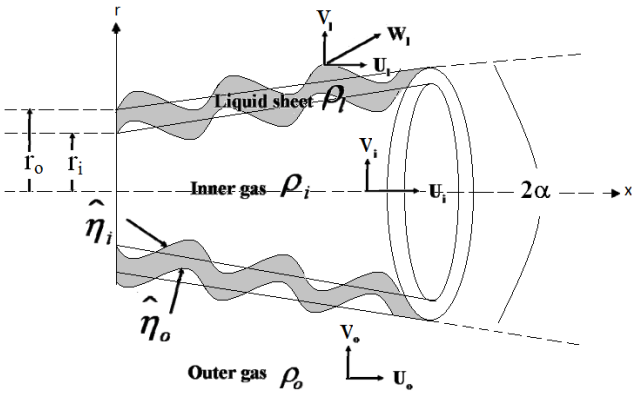

Fig. 1 An annular liquid sheet schematic (current study)

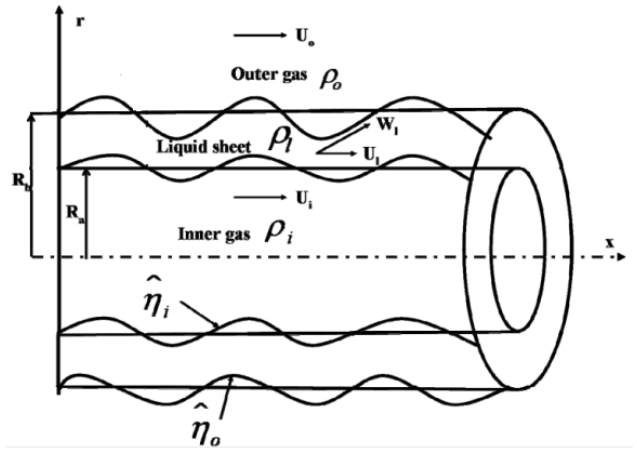

Fig. 2 An annular liquid sheet schematic [14–18]

Velocities of the base flow of liquid sheet (l), inner gas (i) and outer gas (o) in cylindrical coordinates are respectively as (U_l, V_l, A_l/r), (U_i, V_i, 0) and (U_o, V_o, 0). Parameter A_l(m^2/s) is the vortex strength. The vortex strength is measured using a quantity called "Vorticity". This is considered to be at a certain point in the vortex in proportion to the ratio of rotation to surface. Vorticity is a vector quantity that its direction is in the direction of the vortex axis. Also liquid sheet is considered as a free vortex flow.

Pressure forces on the outer and inner surfaces, centrifugal force because of rotation of the sheet, and the surface tension force, which has a favorable effect on the stability of the sheet, are the main forces acting on the liquid sheet. By considering the mentioned assumptions, governing equations (Eqs. (1) and (2)) can be written in the cylindrical coordinate system as follows:

Mass conservation equation:

$$\frac{V}{r}+\frac{\partial V}{\partial r}+\frac{1}{r}\frac{\partial W}{\partial \theta}+\frac{\partial U}{\partial x}=0. \tag{1}$$

Momentum conservation equations:

$$\begin{aligned}
&\frac{\partial U}{\partial t}+V\frac{\partial U}{\partial r}+\frac{W}{r}\frac{\partial U}{\partial \theta}+U\frac{\partial U}{\partial x}=-\frac{1}{\rho}\frac{\partial p}{\partial x}\\
&\frac{\partial V}{\partial t}+V\frac{\partial V}{\partial r}+\frac{W}{r}\frac{\partial V}{\partial \theta}+U\frac{\partial V}{\partial x}-\frac{W^2}{r}=-\frac{1}{\rho}\frac{\partial p}{\partial r}\\
&\frac{\partial W}{\partial t}+V\frac{\partial W}{\partial r}+\frac{W}{r}\frac{\partial W}{\partial \theta}+U\frac{\partial W}{\partial x}-\frac{VW}{r}=-\frac{1}{\rho}\frac{\partial p}{r\partial \theta}.
\end{aligned} \tag{2}$$

To obtain linearized disturbed equations, velocity and pressure components are divided into two parts, including disturbed and mean parts, as below:

$$U=\bar{U}+u, V=\bar{V}+v, W=\bar{W}+w, p=P+p', \tag{3}$$

where prime and over bar are respectively representative of disturbance parameter and mean flow value.

Equation (3) is substituted into the mass conservation and momentum equations (Eqs. (1) and (2)), then the equations of base flow are subtracted. Now linearized disturbed equations (Eq. (4)) relating to the liquid phase are obtained as below:

$$\begin{aligned}
&\frac{v}{r}+\frac{\partial v}{\partial r}+\frac{1}{r}\frac{\partial w}{\partial \theta}+\frac{\partial u}{\partial x}=0\\
&\frac{\partial u}{\partial t}+U_l\frac{\partial u}{\partial x}+V_l\frac{\partial u}{\partial r}+\frac{A_l}{r^2}\frac{\partial u}{\partial \theta}=-\frac{1}{\rho_l}\frac{\partial p_l'}{\partial x}\\
&\frac{\partial v}{\partial t}+U_l\frac{\partial v}{\partial x}+V_l\frac{\partial v}{\partial r}+\frac{A_l}{r^2}\frac{\partial v}{\partial \theta}-\frac{2wA_l}{r^2}=-\frac{1}{\rho_l}\frac{\partial p_l'}{\partial r}\\
&\frac{\partial w}{\partial t}+U_l\frac{\partial w}{\partial x}+V_l\frac{\partial w}{\partial r}+\frac{A_l}{r^2}\frac{\partial w}{\partial \theta}+\frac{V_l w}{r}+\frac{vA_l}{r^2}=-\frac{1}{\rho_l}\frac{\partial p_l'}{r\partial \theta}.
\end{aligned} \tag{4}$$

The linearized disturbed equations (Eq. (5)) relating to the external (o) and internal gas (i) are similarly obtained as below:

$$\begin{aligned}
&\frac{v}{r}+\frac{\partial v}{\partial r}+\frac{1}{r}\frac{\partial w}{\partial \theta}+\frac{\partial u}{\partial x}=0\\
&\frac{\partial u}{\partial t}+U_j\frac{\partial u}{\partial x}+V_j\frac{\partial u}{\partial r}=-\frac{1}{\rho_j}\frac{\partial p_j'}{\partial x}\\
&\frac{\partial v}{\partial t}+U_j\frac{\partial v}{\partial x}+V_j\frac{\partial v}{\partial r}=-\frac{1}{\rho_j}\frac{\partial p_j'}{\partial r}\\
&\frac{\partial w}{\partial t}+U_j\frac{\partial w}{\partial x}+V_j\frac{\partial w}{\partial r}+\frac{V_j w}{r}=-\frac{1}{\rho_j}\frac{\partial p_j'}{r\partial \theta}
\end{aligned} \quad ; \quad j=i,o. \tag{5}$$

Disturbance parameters are presumed as follows:

$$\left(u,v,w,p'\right)=\left(\hat{u}(r),\hat{v}(r),\hat{w}(r),\hat{p}(r)\right)e^{i\left(\frac{k}{\cos\alpha}x+n\theta-\omega t\right)}, \tag{6}$$

where ˆ is indicative of the disturbance amplitude, a function of only r. Parameter α is the half angle of spray cone. The circumferential wave number (n) and axial wave number

($k = 2\pi/\lambda$) are real numbers but frequency $\omega = \omega_r + i\omega_i$ is complex. Maximum amount of imaginary part of the frequency is equal to the disturbance growing rate.

The disturbance displacement in outer and inner interfaces is defined as below:

$$\eta_j(x,r,\theta,t) = \hat{\eta}_j e^{i\left(kx/\cos a + n\theta - \omega t\right)}; \quad j = i,o, \tag{7}$$

where $\hat{\eta}_j$ is a function of x and r. Its components (Fig. 3) in x and r directions are defined as below:

$$\hat{\eta}_{or} = \hat{\eta}_o \cos\alpha,\ \hat{\eta}_{ox} = \hat{\eta}_o \sin\alpha,\ \hat{\eta}_{ir} = \hat{\eta}_i \cos\alpha,\ \hat{\eta}_{ix} = \hat{\eta}_i \sin\alpha. \tag{8}$$

2.1 Boundary conditions on liquid-gas interfaces

2.1.1 Kinematic boundary conditions

The first boundary condition is kinematic boundary condition which must be applied for the outer and inner gas-liquid interfaces. Based on this boundary condition, the vertical velocity components at the interface must remain continuous:

$$\vec{v}_{\xi 1}\vec{n} = \vec{v}_{\xi 2}\vec{n}, \tag{9}$$

where $\vec{v}_{\xi 1}$ and $\vec{v}_{\xi 2}$ are the vectors of local vertical liquid and gas velocity on both interface sides. Also $\vec{n}$ is normal local vector on the interface.

Then the vertical velocity components are decomposed as follows:

$$\left(\vec{v}_1 + \vec{u}_1\right)\vec{n} = \left(\vec{v}_2 + \vec{u}_2\right)\vec{n}, \tag{10}$$

where $\vec{u}_{1,2}$ and $\vec{v}_{1,2}$ are vectors of local velocity (axial and vertical velocity components of liquid and gas) on both interface sides.

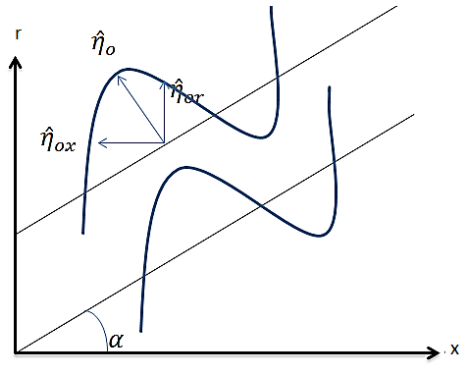

Fig. 3 Disturbance displacement components for a cone-shaped liquid sheet

Therefore, Eq. (11) is adapted from Eq. (9) for the inner interface:

$$\begin{aligned} v_{\xi i} &= \frac{D\eta_i}{Dt} = \frac{\partial\eta_i}{\partial t} + U_i\frac{\partial\eta_i}{\partial x} + V_i\frac{\partial\eta_i}{\partial r}, && r = r_i(x) \\ v_{\xi l} &= \frac{D\eta_i}{Dt} = \frac{\partial\eta_i}{\partial t} + U_l\frac{\partial\eta_i}{\partial x} + V_l\frac{\partial\eta_i}{\partial r} + \frac{A_l}{r^2}\frac{\partial\eta_i}{\partial\theta}, && r = r_i(x), \end{aligned} \tag{11}$$

and for the outer interface can be written as follows:

$$\begin{aligned} v_{\xi o} &= \frac{D\eta_o}{Dt} = \frac{\partial\eta_o}{\partial t} + U_o\frac{\partial\eta_o}{\partial x} + V_o\frac{\partial\eta_o}{\partial r}, && r = r_o(x) \\ v_{\xi l} &= \frac{D\eta_o}{Dt} = \frac{\partial\eta_o}{\partial t} + U_l\frac{\partial\eta_o}{\partial x} + V_l\frac{\partial\eta_o}{\partial r} + \frac{A_l}{r^2}\frac{\partial\eta_o}{\partial\theta}, && r = r_o(x). \end{aligned} \tag{12}$$

2.1.2 Dynamic boundary condition

Dynamic boundary condition expresses balancing of the forces (including the pressure forces, viscous forces and surface tension) acting on the liquid-gas interface both sides as follows:

$$\left(p_l' - p_j'\right) = \sigma k + \left(\vec{\tau}_l - \vec{\tau}_j\right)\vec{n} + \rho_j\frac{\omega_j^2}{r_j}\eta_j - \rho_l\frac{\omega_l^2}{r_j}\eta_j, \quad j = i,o, \tag{13}$$

where σ is surface tension, k is surface curvature and τ is viscous shear stress. In continuance, Eq. (14) for both outer and inner interfaces can be obtained by ignoring viscosity and substituting k and $\vec{n}$ in Eq. (13):

$$\begin{aligned} \left(p_l' - p_i'\right) &= -\sigma\left(\frac{\partial^2\eta_i}{\partial x^2} + \frac{1}{r_i^2}\frac{\partial^2\eta_i}{\partial\theta^2} + \frac{\eta_i}{r_i^2}\right) - \rho_l\frac{A_l^2}{r_i^3}\eta_i \\ \left(p_l' - p_o'\right) &= -\sigma\left(\frac{\partial^2\eta_o}{\partial x^2} + \frac{1}{r_o^2}\frac{\partial^2\eta_o}{\partial\theta^2} + \frac{\eta_o}{r_o^2}\right) - \rho_l\frac{A_l^2}{r_o^3}\eta_o. \end{aligned} \tag{14}$$

Equations (6) and (7) are substituted into Eq. (14) and Eq. (15) are extracted:

$$\begin{aligned} \left(\hat{p}_l - \hat{p}_i\right) &= \sigma\left(\frac{1}{r_i^2} - \frac{k^2}{\cos^2\alpha} - \frac{n^2}{r_i^2}\right)\hat{\eta}_i - \rho_l\frac{A_l^2}{r_i^3}\hat{\eta}_i \\ \left(\hat{p}_l - \hat{p}_o\right) &= \sigma\left(\frac{1}{r_o^2} - \frac{k^2}{\cos^2\alpha} - \frac{n^2}{r_o^2}\right)\hat{\eta}_i - \rho_l\frac{A_l^2}{r_o^3}\hat{\eta}_o. \end{aligned} \tag{15}$$

2.2 Pressure disturbances of the liquid sheet

Pressure disturbances of the liquid sheet can be calculated by solving Eq. (4). Equation (6) is substituted into Eq. (4) and some algebraic manipulations are performed for them. Equation (16) is consequently obtained:

$$\frac{\hat{v}}{r}+\frac{\partial\hat{v}}{\partial r}+\frac{1}{r}(in)\hat{\omega}+ik'\hat{u}=0$$
$$\frac{1}{k'}\left(-\omega+k'U_l+\frac{nA_l}{r^2}\right)\hat{u}+\frac{1}{ik'}V_l\frac{\partial\hat{u}}{\partial r}=-\frac{1}{\rho_l}\hat{p}_l$$
$$i\left(-\omega+k'U_l+\frac{nA_l}{r^2}\right)\hat{v}+V_l\frac{\partial\hat{v}}{\partial r}-\frac{2A_l}{r^2}\hat{\omega}=-\frac{1}{\rho_l}\frac{\partial p_l'}{\partial r} \qquad (16)$$
$$\frac{r}{in}\left(-\omega+k'U_l+\frac{nA_l}{r^2}\right)\hat{\omega}+\frac{r}{in}\frac{V_l}{r}+\frac{r}{in}V_l\frac{\partial\hat{\omega}}{\partial r}+\frac{r}{in}\frac{A_l}{r^2}\hat{v}$$
$$=-\frac{1}{\rho_l}\hat{p}_l,$$

where:

$$k'=\frac{k}{\cos\alpha}. \qquad (17)$$

Parameters $\hat{p}$ and $\hat{u},\hat{v},\hat{\omega}$ should be derived from Eq. (16). Equation (16) are manipulated and, therefore, Eq. (18) can be resulted to derive the parameters $\hat{u}$, $\hat{v}$, $\hat{\omega}$:

$$\frac{\hat{v}}{r}+\frac{\partial\hat{v}}{\partial r}+\frac{1}{r}(in)\hat{\omega}+ik'\hat{u}=0$$
$$\frac{1}{k'}\left(-\omega+k'U_l+\frac{nA_l}{r^2}\right)\hat{u}+\frac{1}{ik'}V_l$$
$$=\frac{r}{in}\left(-\omega+k'U_l+\frac{nA_l}{r^2}\right)\hat{\omega}+\frac{r}{in}\frac{V_l}{r}+\frac{r}{in}V_l\frac{\partial\hat{\omega}}{\partial r}+\frac{r}{in}\frac{A_l}{r^2}\hat{v}\frac{\partial\hat{u}}{\partial r}$$
$$\frac{1}{k'}\left(-\omega+k'U_l+\frac{nA_l}{r^2}\right)\frac{\partial\hat{u}}{\partial r}+\frac{1}{ik'}V_l\frac{\partial^2\hat{u}}{\partial r^2}$$
$$=i\left(-\omega+k'U_l+\frac{nA_l}{r^2}\right)\hat{v}+V_l\frac{\partial\hat{v}}{\partial r}-\frac{2A_l}{r^2}\hat{\omega}.$$
(18)

After obtaining the parameters of $\hat{u}$, $\hat{v}$, $\hat{\omega}$ and substituting them into the second equation of Eq. (16) $\hat{p}$ can also be obtained.

2.3 Pressure disturbances of the external and internal gas flows

The disturbances of pressure in the internal and external gases can be obtained by solving Eq. (5). Linearised disturbed equation can be obtained by substitution of Eq. (6) in Eq. (5) and some algebraic simplifications:

$$\frac{\hat{v}}{r}+\frac{\partial\hat{v}}{\partial r}+\frac{1}{r}(in)\hat{\omega}+ik'\hat{u}=0$$
$$\frac{1}{ik'}\left[\left(-i\omega+ik'U_j\right)\hat{u}+V_j\frac{\partial\hat{u}}{\partial r}\right]=-\frac{1}{\rho_j}\hat{p}_j$$
$$i\left(-\omega+k'U_j\right)\hat{v}+V_j\frac{\partial\hat{v}}{\partial r}=-\frac{1}{\rho_j}\frac{\partial p_j'}{\partial r} \quad ; \quad j=i,o.$$
$$\frac{r}{in}\left(\left(-i\omega+ik'U_j\right)\hat{\omega}+V_j\frac{\partial\hat{\omega}}{\partial r}+\frac{V_j\hat{\omega}}{r}\right)=-\frac{1}{\rho_j}\hat{p}_j$$
(19)

The external and internal gas equations are similar to each other. Similar to the liquid sheet equations (Eqs. (18) and (20)), Eq. (20) is set up to calculate the disturbance parameters of velocity:

$$\frac{\hat{v}}{r}+\frac{\partial\hat{v}}{\partial r}+\frac{1}{r}(in)\hat{\omega}+ik'\hat{u}=0$$
$$\frac{1}{ik'}\left[\left(-\omega i+ik'U_i\right)\hat{u}+V_i\frac{\partial\hat{u}}{\partial r}\right]$$
$$=\frac{r}{ni}\left(\left(-i\omega+ik'U_i\right)\hat{\omega}+V_i\frac{\partial\hat{\omega}}{\partial r}+\frac{V_i\hat{\omega}}{r}\right)$$
$$\frac{1}{ik'}\left[\left(-\omega i+ik'U_i\right)\frac{\partial\hat{u}}{\partial r}+V_i\frac{\partial^2\hat{u}}{\partial r^2}\right]=i\left(-\omega+k'U_i\right)\hat{v}+V_i\frac{\partial\hat{v}}{\partial r}.$$
(20)

Equation (20) can be applied to achieve the disturbance velocity components to determine pressure disturbances using one of momentum equations of Eq. (19) as the next step. Final equation will be derived by substituting internal and external gas and liquid sheet pressure disturbances, obtained from Subsections 2.2 and 2.3, in Eq. (15) and then eliminating $\hat{\eta}_i,\hat{\eta}_o$.

Both in the current analysis and in Ibrahim linear stability analysis, linear stability theory has been implemented but these two analyses are not the same in the governing equations. Some additional parameters such as cone angle and radial velocities are considered in the current analysis (in comparison with Ibrahim linear stability analysis) to add the effects of being cone-shaped in the stability analysis. Hereupon the mathematical formulation became so complicated that it could not be solved analytically. It should be noted that in the prior analyses, the cone angle and components of radial velocity were ignored in governing equations, therefore, the mathematical formulation was neat.

2.4 Calculation of the wave characteristics

For estimation of the wave characteristics, pressure disturbances of the liquid sheet, external and internal gas flows, presented previously, are substituted in Eq. (15) and then final equation can be obtained by omitting $\hat{\eta}_i,\hat{\eta}_o$. The following dimensionless parameters introduced in Eq. (21) were defined to investigate the effects of different items such as properties of fluids, geometrical parameters and forces. By introducing these dimensionless parameters final equation can be non-dimensionalized. Though, investigation of the effect of these dimensionless parameters is not the objective of the current study.

$$\begin{aligned}
&\mathrm{We}_{ix}=\frac{\rho_i U_i^2 R_b}{\sigma},\ \mathrm{We}_{ox}=\frac{\rho_o U_o^2 R_b}{\sigma},\ \mathrm{We}_{lx}=\frac{\rho_l U_l^2 R_b}{\sigma},\\
&\mathrm{We}_{ir}=\frac{\rho_i V_i^2 R_b}{\sigma},\ \mathrm{We}_{or}=\frac{\rho_o V_o^2 R_b}{\sigma},\\
&\mathrm{We}_{lr}=\frac{\rho_l V_l^2 R_b}{\sigma},\ \mathrm{We}_{ls}=\frac{\rho_l A_l^2}{\sigma R_b},\ g_i=\frac{\rho_i}{\rho_l},\ g_o=\frac{\rho_o}{\rho_l},\\
&h=\frac{R_a}{R_b},\ \bar{k}=kR_b,\ \bar{\omega}=\frac{\omega R_b}{U_l}
\end{aligned} \tag{21}$$

The extended form of final non-dimensional equation (full equation) will be too complex. But it can be prepared in a generalized form. Parameter $\bar{\omega}$ is unknown. The wave number corresponding to the maximum growing rate, called the most unstable wave number, is obtained by solving Eq. (22).

$$f\begin{pmatrix}\bar{\omega},\ \bar{k},\ \alpha,\ h,\ g_i,\ g_o,\ \mathrm{We}_{ix},\ \mathrm{We}_{ox},\\ \mathrm{We}_{lx},\ \mathrm{We}_{ir},\ \mathrm{We}_{or},\ \mathrm{We}_{lr},\ \mathrm{We}_{ls}\end{pmatrix}=0 \tag{22}$$

Final dispersion equation (Eq. (22)) was solved numerically by Maple™. To solve the final equation, parameters of ρ_i, U_i, V_i, ρ_l, U_l, V_l, A_l, ρ_o, U_o, V_o, R_b, R_a, σ, $\bar{k}$, α, n were used as input parameters.

2.5 Prediction of the breakup length

Breakup length (L_b) and initial drop diameter (d_D) are estimated using Eqs. (23) and (24) [23]. Parameters of $\bar{\omega}$ and corresponding $\bar{k}$ should be substituted into Eqs. (23) and (24):

$$L_b=\frac{12R_b}{\bar{\omega}}, \tag{23}$$

$$d_D=1.88d_L\left(1+3\mathrm{Oh}\right)^{1/6}, \tag{24}$$

where $\mathrm{Oh}=\mu_l/(\rho_l\sigma d_L)^{1/2}$ and $d_l=\sqrt{16h_sR_b/\bar{K}}$. Also ρ_l is density and μ_l is viscosity of the liquid. In the current study, it is assumed that there is no viscous force, therefore, Ohnesorge number (Oh) is considered to be zero.

3 Results and discussions

Previous experimental and analytical studies done on the liquid jets with the involvement of the external and internal gas with similar specifications were considered to validate the analysis [14, 24, 25]. The procedure implemented here is in a way that makes it possible to solve the liquid sheet governing equations (Eq. (16)) for wide variety of cone angles, larger than 0 degrees and less than 180 degrees.

Current analysis results for a cylindrical liquid jet (i.e. cone-shaped spray angle equal to zero) and analytical results of Ibrahim [14] are compared with each other in Fig. 4 to approve the good accuracy of the current work. Fig. 4 displays growing rate versus wave number of the liquid sheet. As can be seen in Fig. 4, the curves of growing rate in terms of wave number, resulted from the current study and Ibrahim linear stability analysis, are wholly congruous with each other. In this case study, cone angle was set to be zero to compare Ibrahim linear stability analysis with the current study results. This curve proves that the proposed analysis enables to generate the equivalent results for zero-angle liquid jets. From now on, the cone angle is considered in the model of instability through the proposed implementation of linear stability theory.

Fig. 5 shows the results of the proposed implementation for a cone-shaped jet in comparison with the experimental data measured by Bruce [24]. This curves shows the proposed procedure capability to model the instability in annular cone-shaped sprays. To show the suitable capability of proposed implementation, a similar parallel assessment was performed using linear stability analysis of Ibrahim [14]. Fig. 5 illustrates that general stability analysis cannot precisely capture cone-shaped spray instability. However, the current study can properly calculate the axial wave number and maximum growing rate. Hence, the mean droplet diameter and breakup length can be predicted further accurately. The variance observed between the two results is because of difference in the governing equations. In the current analysis, the effect of cone angle has been considered and governing equations

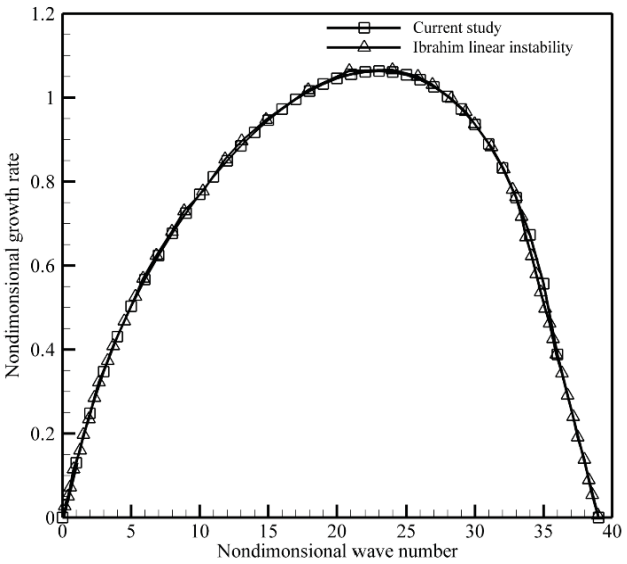

Fig. 4 Comparison of the results of proposed procedure for a cylindrical liquid jet (i.e. zero angle cone-shaped spray) and Ibrahim analytical data published by for a cylindrical liquid jet [14], $\mathrm{We}_{lx}=10^{-4}$, $\mathrm{We}_{ix}=0$, $\mathrm{We}_{ox}=70$, $\mathrm{We}_{ls}=500$, $\mathrm{We}_{is}=\mathrm{We}_{os}=500$, $g_i=g_o=0.00123$, $h=0.677$, $n=0$

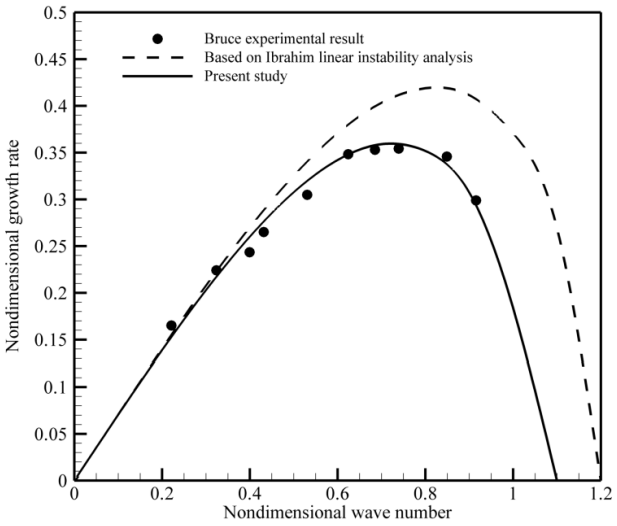

Fig. 5 Comparison of the results of the proposed implementation for a cone-shaped jet and the experimental data measured by Ibrahim [14] and Bruce [24] stability analysis, Re = 169, d_n = 0.02 mm, ρ_l = 1022 g/l, μ_l = 0,00262 pa, σ = 0.05 kg/s^2

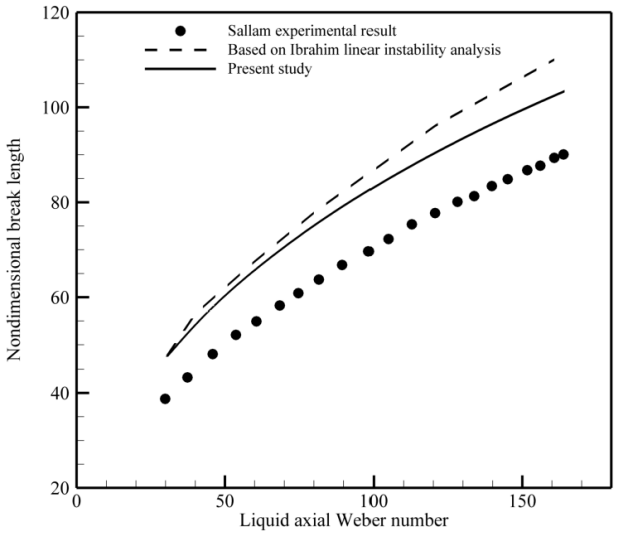

Fig. 6 Comparison of predicted breakup length in terms of liquid axial Weber number with Ibrahim [14] experiment and Sallam et al. [25] stability analysis, n = 0, We$_{lx}$ = 30, We$_{ls}$ = We$_{is}$ = We$_{ox}$ = 0, R_o = 1.9 µm, σ = 0.072 kg/s^2, ρ_l = 997 kg/m^3

have been written for a hollow cone-shaped liquid sheet, whereas the classic analysis could not reflect the cone angle effect and it can just be used for a zero-angle liquid sheet (cylindrical). The outcomes demonstrate that cone angles have a strong effect on the most unstable disturbance (Fig. 5) and show the good potency of the proposed implementation procedure to guess instability characteristics.

Fig. 6 presents the non-dimensional breakup length predicted by the presented method in terms of the axial Weber number of liquid jet. Fig. 6 was presented in order to inspect the capability of the proposed implementation of linear stability theory in estimation of breakup length. It displays result of the current linear stability analysis compared with experimental data of Sallam et al. [25] and the breakup length predicted by linear stability analysis of Ibrahim [14]. The results and the experimental data show a good agreement with each other that it can be considered as a re-verification for this study. Moreover, it can be observed that the distance between the two curves (bullet and dashed line) becomes more when liquid axial Weber number increases, but the present result (solid line) follows up the rising trend with the same slope but a smaller distance towards the experimental data. Fig. 6 shows that the non-dimensional breakup length in terms of the liquid sheet axial Weber number obtained by the new linear stability analysis (present study) is closer to experimental data of Sallam et al. [25] than that obtained based on linear stability analysis of Ibrahim [14].

Nevertheless, a not so little discrepancy can be seen between the experimental data and the new model results in Fig. 6. The reason is the weakness of Eq. (23) available from the literature to estimate the breakup length. This simple equation (Eq. (23)) was defined using a simple criterion based on large experiments as follows and used up to now:

$$\ln\left(\frac{\eta_{\text{breakup}}}{\eta_{\text{initial}}}\right)=12 \tag{25}$$

where parameter η is the wave amplitude. Because of the fact that Eq. (23) has been presented using the simple criterion of Eq. (25), therefore, it is clear that accuracy of the breakup length and consequently mean droplet diameter calculations will be affected by this formulation, however, prediction of the wave characteristics is high accuracy. Enhancing this formulation to strongly predict the breakup length requires hard work in the future.

In a parallel study, a centrifugal injector with four tangential inlets, as introduced in Table 1, was designed and successfully tested. Its half angle of spray is 55 degrees. The proposed analysis was used to assess physical characteristics of the wave for the mentioned injector Fig. 7 displays wave growing rates versus wave number. Using Fig. 7 some parameters mandatory to predict initial drop diameter (d_D) and breakup length (L_b) are prepared. These amounts are presented in Table 2.

To assess the influence of cone angle on the instability relating to the mentioned injector, another work was

Table 1 Spray characteristics

Parameter	Value
Liquid Density	998.2 (Kg/m^3)
Gas Density	1.22 (Kg/m^3)
Ambient Pressure	1 (bar)
Surface Tension	0.073 (N/m)
Flow Rate	0.06 (Kg/s)
Nozzle Radius	2 mm
Liquid Average Velocity	12.8 (m/s)
Cone Half Angle	55 degrees

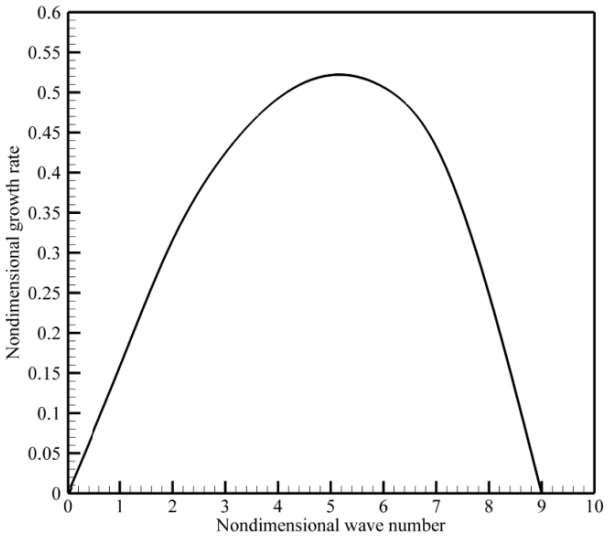

Fig. 7 Growing rate versus wave number of liquid sheet with cone half angle of 55 degrees predicted by proposed implementation. $We_{lx} = 4479$, $We_{ix} = 0.83$, $We_{ox} = 0$, $We_{ls} = 174$, $We_{is} = We_{os} = 0$, $g_i = g_o = 0.00122$, $h = 0.8$, $n = 0$

Table 2 Obtained information by the stability analysis

Wave Number	Maximum Growth Rate	Breakup Length (mm)	Reynolds Number	Weber Number
5	0.5215	46.02	20000	4479

correspondingly done. One of the important problems in combustion chamber design is limitation of available space and/or weight. As quoted earlier, the proposed analysis can solve liquid sheet governing equations (Eq. (16)) for wide angle variety. The diagram of non-dimensional growing rate in terms of non-dimensional axial wave number for some diverse cone angles are presented in Fig. 8. As can be observed, maximum growing rate rises when the cone angle becomes larger, and corresponding frequency or most unstable wave number declines to minor level. These changes in the growing rates and most unstable wave numbers point out that the cone angle has

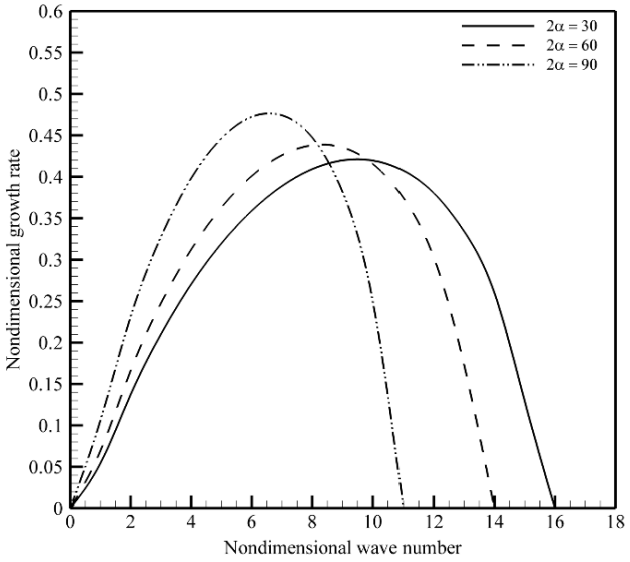

Fig. 8 Non-dimensional growing rate in terms of non-dimensional axial wave number in liquid sheet for some diverse cone angles, $We_{lx} = 4479$, $We_{ix} = 0.83$, $We_{ox} = 0$, $We_{ls} = 174$, $We_{is} = We_{os} = 0$, $g_i = g_o = 0.00122$, $h = 0.8$, $n = 0$

a significant impact on the breakup length and produced droplet diameter. In fact, the higher cone angles intensify the liquid sheet instability and consequently can lead to smaller breakup length, bigger filaments and droplets. Experimental observations confirm this behavior.

The influence of cone angle on the breakup length of a cone-shaped liquid sheet for wide variety of cone angles is illuminated in Fig. 9. The curve slope rises with growth in cone angle because of intensification of aerodynamic interaction between gas flows and liquid sheet.

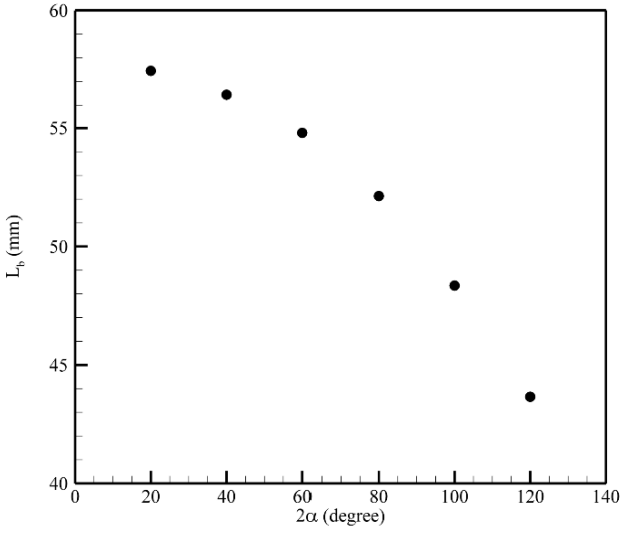

Fig. 9 Breakup length in terms of cone angle of liquid sheet $We_{lx} = 4479$, $We_{ix} = 0.83$, $We_{ox} = 0$, $We_{ls} = 174$, $We_{is} = We_{os} = 0$, $g_i = g_o = 0.00122$, $h = 0.8$, $n = 0$

Considering cone angle is important in the area before breakup for sprays that have relatively long breakup length (millimetric order). The more cone angle causes the more significant effects in the stability model. Therefore, regardless of the cone angle effect can cause the inaccuracy in estimation of the relevant characteristics. The proposed model can support us to further truthfully implement the stability theory on cone-shaped sprays.

4 Conclusions

To determine the mass mean diameter of resulting droplets and the breakup length of spray, the instability of a hollow cone-shaped liquid sheet generated by centrifugal injector was investigated. Using the hydrodynamic stability theory, a numerical model was developed with regard to the three-dimensional effects of the gas and liquid flows to predict the instability of an inviscid swirling cone-shaped liquid sheet in presence of the external and internal gas flows. The numerical model developed in the current work makes available an opportunity to solve the liquid sheet governing equations for wide variety of cone angles.

Cone angle and its effects on stability of the liquid sheet is vital issue in design of combustion chambers because of the limitation of the available space and/or weight. The maximum growing rate growths when the cone angle becomes larger and corresponding frequency or most unstable wave number declines to minor level. These changes in the growing rates and most unstable wave numbers point out that the cone angle has a significant impact on the breakup length and produced droplet diameter. In fact, the higher cone angles intensify the liquid sheet instability and consequently can lead to smaller breakup length, bigger filaments and droplets. Experimental observations confirm this behavior. Implementation of linear stability theory on a hollow cone-shaped liquid sheet (the current analysis) better can predict instability in comparison with the general linear stability model. The current model can deepen knowledge of modeling of instability and can help designers of combustion chambers as a strong tool in different industries.

Nomenclature

A_l	Vortex Strength (m^2/s)
d_D	Droplet diameter
d_L	Filament diameter
g	Gas-to-liquid density ratio
h_c	Characteristic length
h	Ratio of inner and outer radius
i	Imaginary unit
k	Axial wave number (1/m)
L_b	Breakup length
n	Circumferential wave number (1/Rad)
p'	Disturbance pressure (N/m^2)
P	Mean pressure (N/m^2)
Re	Reynolds number $\rho U^2 h_c / \mu$
R_a	Inner diameter of liquid sheet (m)
R_b	Outer diameter of liquid sheet (m)
u	Disturbance axial velocity (m/s)
U	Mean axial velocity (m/s)
v	Disturbance radial velocity (m/s)
V	Mean radial velocity (m/s)
w	Disturbance tangential velocity (m/s)
We	Weber number $\rho U^2 R_b / \sigma$
W	Mean tangential velocity (m/s)
σ	Surface tension (kg/s^2)
η	Displacement disturbance (m)
μ	Dynamic viscosity
ρ	Density
ω	Temporal growing rate (1/s)

Subscripts

i/o	Internal gas/External gas
l	Liquid

References

[1] Fritsching, U. "Spray Simulation: Modeling and Numerical Simulation of Spray Forming metals", Cambridge University Press, Cambridge, UK, 2004. https://doi.org/10.1017/CBO9780511536649

[2] Ashgriz, N. "Handbook of Atomization and Sprays: Theory and Applications", Springer Science & Business Media, Springer, Boston, MA, USA, 2011. https://doi.org/10.1007/978-1-4419-7264-4

[3] Lord Rayleigh, F. R. S. "On The Instability of Jets", Proceedings of the London Mathematical Society, s1–10(1), pp. 4–13, 1878. https://doi.org/10.1112/plms/s1-10.1.4

[4] Crapper, G. D., Dombrowski, N., Pyott, G. A. D. "Kelvin–Helmholtz wave growth on cylindrical sheets", Journal of Fluid Mechanics, 68(3), pp. 497–502, 1975. https://doi.org/10.1017/S0022112075001784

[5] Shen, J., Li, X. "Instability of an annular viscous liquid jet", Acta Mechanica, 114(1), pp. 167–183, 1996. https://doi.org/10.1007/BF01170402

[6] Panchagnula, M. V., Sojka, P. E., Santangelo, P. J. "On the three-dimensional instability of a swirling, annular, inviscid liquid sheet subject to unequal gas velocities", Physics of Fluids, 8(12), pp. 3300–3312, 1996. https://doi.org/10.1063/1.869119

[7] Jeandel, X., Dumouchel, C. "Influence of the viscosity on the linear stability of an annular liquid sheet", International Journal of Heat and Fluid Flow, 20(5), pp. 499–506, 1999. https://doi.org/10.1016/S0142-727X(99)00038-7

[8] Jazayeri, S. A., Li, X. "Structure of Liquid-Sheet Sprays", Particle & Particle Systems Characterization, 17(2), pp. 56–65, 2000. https://doi.org/10.1002/1521-4117(200006)17:2<56::AID-PPSC56>3.0.CO;2-0

[9] Chin, J. S., Rizk, N. K., Razdan, M. K. "Effect of Inner and Outer Airflow Characteristics on High Liquid Pressure Prefilming Airblast Atomization", Journal of Propulsion and Power, 16(2), pp. 297–301, 2000. https://doi.org/10.2514/2.5568

[10] Sirignano, W. A., Mehring, C. "Review of theory of distortion and disintegration of liquid streams", Progress in Energy and Combustion Science, 26(4–6), pp. 609–655, 2000. https://doi.org/10.1016/S0360-1285(00)00014-9

[11] Lin, S. P. "Breakup of Liquid Sheets and Jets", Cambridge University Press, Cambridge, UK, 2003. https://doi.org/10.1017/CBO9780511547096

[12] Cao, J. "Theoretical and experimental study of atomization from an annular liquid sheet", Proceedings of the Institution of Mechanical Engineers, Part D: Journal of Automobile Engineering, 217(8), pp. 735–743, 2003. https://doi.org/10.1243/09544070360692122

[13] Du, Q., Li, X. "Effect of gas stream swirls on the instability of viscous annular liquid jets", Acta Mechanica, 176(1), pp. 61–81, 2005. https://doi.org/10.1007/s00707-004-0183-1

[14] Ibrahim, A. "Comprehensive study of internal flow field and linear and nonlinear instability of an annular liquid sheet emanating from an atomizer", Doctoral dissertation, University of Cincinnati, 2006.

[15] Ibrahim, A. A., Jog, M. A. "Nonlinear instability of an annular liquid sheet exposed to gas flow", International Journal of Multiphase Flow, 34(7), pp. 647–664, 2008. https://doi.org/10.1016/j.ijmultiphaseflow.2007.12.003

[16] Sahu, K. C., Matar, O. K. "Three-dimensional linear instability in pressure-driven two-layer channel flow of a Newtonian and a Herschel-Bulkley fluid", Physics of Fluids, 22(11), Article Number: 112103, 2010. https://doi.org/10.1063/1.3502023

[17] Yan, K., Jog, M. A., Ning, Z. "Nonlinear spatial instability of an annular swirling viscous liquid sheet", Acta Mechanica, 224(12), pp. 3071–3090, 2013. https://doi.org/10.1007/s00707-013-0896-0

[18] Mahdavi, S. A., Movahednejad, E., Ommi, F., Hosseinalipour, S. M. "Estimation of the Breakup Length for the Annular and the Round Liquid Jet Using Linear Instability Analysis", Iranian Journal of Science and Technology: Transactions of Mechanical Engineering, 37(2), pp. 217–232, 2013. https://doi.org/10.22099/IJSTM.2013.1749

[19] Fu, Q. F., Yang, L. J., Qu, Y. Y., Gu, B. "Linear Stability Analysis of a Conical Liquid Sheet", Journal of Propulsion and Power, 26(5), pp. 955–968, 2010. https://doi.org/10.2514/1.48346

[20] Sahu, K. C., Govindarajan, R. "Linear stability analysis and direct numerical simulation of two-layer channel flow", Journal of Fluid Mechanics, 798, pp. 889–909, 2016. https://doi.org/10.1017/jfm.2016.346

[21] Liao, Y., Jeng, S. M., Jog, M. A., Benjamin, M. A. "Advanced Sub-Model for Airblast Atomizers", Journal of Propulsion and Power, 17(2), pp. 411–417, 2001. https://doi.org/10.2514/2.5757

[22] Gordillo, J. M., Pérez-Saborid, M. "Aerodynamic effects in the break-up of liquid jets: on the first wind-induced break-up regime", Journal of Fluid Mechanics, 541, pp. 1–20, 2005. https://doi.org/10.1017/S0022112005006026

[23] Senecal, P. K., Schmidt, D. P., Nouar, I., Rutland, C. J., Reitz, R. D., Corradini, M. L. "Modeling high-speed viscous liquid sheet atomization", International Journal of Multiphase Flow, 25(6–7), pp. 1073–1097, 1999. https://doi.org/10.1016/S0301-9322(99)00057-9

[24] Bruce, C. A. "Dependence of Ink Jet Dynamics on Fluid Characteristics", IBM Journal of Research and Development, 20(3), pp. 258–270, 1976. https://doi.org/10.1147/rd.203.0258

[25] Sallam, K. A., Dai, Z., Faeth, G. M. "Liquid breakup at the surface of turbulent round liquid jets in still gases", International Journal of Multiphase Flow, 28(3), pp. 427–449, 2002. https://doi.org/10.1016/S0301-9322(01)00067-2